

Newcastle University

Evaluation of Heterogeneous Quaternary Ammonium Catalysts for Transesterification of Triglycerides

A thesis submitted to the Newcastle University for the degree
of Doctor of Philosophy

by

Wan Mohd Hafizuddin Wan Yussof

School of Chemical Engineering and Advanced Materials,
Newcastle University

March 2012

PERPUSTAKAAN UNIVERSITI MALAYSIA PAHANG	
No. Perolehan 064553	No. Panggilan TP 339 B46 H34 2012 RS
Tarikh 30 APR 2012	

Abstract

Biodiesel is a mixture of an alkyl ester of long chain fatty acids produced by transesterification of triglycerides with lower alcohols such as methanol, in the presence of acid or base catalysts. Nearly all biodiesel processes use homogeneous base catalysts that cannot be recovered and necessitate neutralisation of the glycerol-rich phase (a by-product of the reaction). This increases the number of downstream separation steps, thereby increasing the capital cost of biodiesel production processes. Replacing liquid homogeneous catalysts with solid heterogeneous catalysts can intensify the process, by reducing the total number of process steps, eliminate or reduce waste streams and result in lower production costs, as the catalyst will not have to be continually replaced.

Strong anion exchange resins with QN^+OH^- , have the potential to be developed and employed as heterogeneous catalyst for transesterification, as they are chemically stable to leaching of the functional group. In this present work, nine different synthesized anion exchange resins (SIER1-9) were prepared by suspension polymerization of vinylbenzyl chloride-divinylbenzene (VBC-DVB) copolymers in the presence of n-heptane as a pore-forming agent. These SIERs were evaluated as catalysts for transesterification of triacetin. It was found that the “SIER-6” catalyst prepared with the highest dilution degree (200%) and the lowest DVB content (10% DVB), achieved the highest triacetin conversion (95.6% after 4h). This catalyst had the highest true pore volume ($0.89 \text{ cm}^3/\text{g}$) and surface area ($398.8 \text{ m}^2/\text{g}$). In contrast, the “SIER-7” catalyst synthesized with the lowest dilution degree (50%), but highest DVB content (40%), resulted in the lowest triacetin conversion at 64.3%. Although there is a considerable improvement in the physicochemical properties of the IERs, such as surface area, ‘true pore’ volume and diameter, transesterification using rapeseed oil was rather poor with only 16 wt. % of FAME obtained over SIER-6 after 6h reaction.

Overall, the ion exchange resin-catalyzed reaction were well-described by the Eley-Rideal model. Significantly, the ER model data fitted the experimental data for all ion exchange resins studied in this work.

Table of Contents

Abstract.....	ii
Acknowledgements	iii
Table of Contents	iv
List of Figures.....	viii
List of Tables.....	xii
Nomenclature and Abbreviations	xiii
INTRODUCTION.....	1
1.1 Background: Biofuels	1
1.2 The Use of Vegetable Oils.....	4
1.3 Intensified Biodiesel Process Using Heterogeneous Catalyst.....	6
1.4 Research Objective	9
1.5 Research Scope	9
LITERATURE REVIEW	10
2.1 Introduction.....	10
2.2 Sources of Triglycerides	10
2.2.1 Rapeseed Oil.....	10
2.2.2 Triacetin.....	12
2.3 The Chemistry of Biodiesel Production.....	14
2.3.1 Transesterification	14
2.3.2 Esterification.....	16
2.3.3 Technologies of Biodiesel Production.....	17
2.4 Catalyst Application in Biodiesel Production.....	18
2.4.1 Homogeneous Catalysts	19
2.4.1.1 Alkaline Catalysts	19
2.4.1.2 Acid Catalysts	23
2.4.2 Heterogeneous Catalysts	25
2.4.2.1 Heterogeneous Alkaline Catalysts	26
2.4.2.2 Acid Catalysts	30
2.4.3 Enzyme Catalysts	32
2.4.4 Anionic Exchange Resins.....	33
2.4.5 Summary.....	35
2.5 Synthesized Ion Exchange Resins (SIERs).....	36
2.5.1 Suspension Polymerization of Styrene-Divinylbenzene (S-DVB).....	36
2.5.2 Factors Affecting Pore Formation in Suspension Polymerization	38
2.5.3 Chloromethylation and the Functionalization of S-DVB Copolymers	42

2.5.4	Summary.....	44
2.6	The Kinetic Modelling of Transesterification.....	45
2.6.1	Second-Order Kinetics Model.....	46
2.6.2	Model Construction.....	50
2.6.2.1	Langmuir-Hinshelwood-Hougen-Watson (LHHW) Model.....	52
2.6.2.2	Eley-Rideal (ER) Model.....	56
2.6.3	Diffusional Resistance.....	58
MATERIALS AND METHODS		61
3.1	Introduction.....	61
3.2	Evaluation of Quaternary Ammonium Ion Exchange Resin as Heterogeneous Transesterification Catalysts for Rapeseed Oil.....	61
3.2.1	Amberlite™ A26.....	62
3.2.2	Effect of Catalyst Concentration.....	62
3.2.3	Analysis of Free Fatty Acids in Rapeseed Oil.....	63
3.2.4	Effect of Pre-Swelling the Amberlite™ A26.....	63
3.3	Gas Chromatography (GC) Analysis.....	64
3.3.1	Determination of Ester Content in Rapeseed Oil.....	64
3.3.2	Sample Preparation.....	64
3.3.3	Ester Content Calculation.....	64
3.3.4	Determination of Ester Content in Triacetin.....	65
3.3.5	GC Calibration Curve for Triacetin Analysis.....	66
3.4	Transesterification of Triacetin using Quaternary Ammonium Catalysts.....	67
3.4.1	Effect of Stirring Speed.....	69
3.4.2	Effect of Temperature.....	69
3.4.3	Effect of Catalyst Concentration.....	69
3.4.4	Effect of Particle Size.....	69
3.4.5	Reusability and Residual Activity Studies.....	69
3.5	Catalyst Characterization.....	71
3.5.1	Elemental Analysis.....	71
3.5.2	FTIR-ATR Analysis.....	71
3.5.3	Ion Exchange Capacity.....	71
3.5.4	Apparent Density.....	73
3.5.5	SEM Analysis.....	74
3.5.6	NMR Analysis.....	74
3.5.7	Thermal Gravimetric Analysis (TGA).....	75
3.5.8	Surface Area Analysis by the BET Method.....	75
3.5.9	Assessment of the Ion Exchange Resin Porosity in Swollen State.....	75

3.6	Synthesis of Ion Exchange Resins (SIERs)	78
3.6.1	Initial Synthesis of S-DVB Copolymers	78
3.6.2	Direct Chloromethylation of S-DVB Copolymers	79
3.6.3	Amination of Merrifield Resins and S-DVB Copolymers	80
3.6.3.1	Amination with Triethylamine (TEA).....	80
3.6.3.2	Amination with Trimethylamine (TMA)	80
3.6.4	Transesterification of SIERs with Triacetin	81
3.7	Transesterification Using Rapeseed Oil.....	81
RESULTS AND DISCUSSION.....		82
4.1	Analytical Method Development.....	82
4.1.1	GC Analysis of Ester Content of Rapeseed Oil.....	82
4.1.2	GC Analysis of Ester Content of Triacetin.....	83
4.2	Evaluation of Quaternary Ammonium Ion Exchange Resin as a Heterogeneous Transesterification Catalyst for Rapeseed Oil	87
4.2.1	Amberlite™ A26	87
4.2.2	Effect of Pre-Swelling the Amberlite™ A26	89
4.2.3	Summary.....	91
4.3	Quaternary Ammonium as Transesterification Catalysts	91
4.3.1	Evaluation of Heterogeneous Quaternary Ammonium IERs	92
4.3.2	Characterization of Ion Exchange Resins (IERs).....	94
4.3.3	Reusability and Residual Activity	97
4.3.4	Evaluation of Homogeneous Quaternary Ammonium Catalysts	100
4.3.5	Summary.....	105
4.4	Merrifield Resin	106
4.4.1	Introduction	106
4.4.2	Amination of Merrifield Resin	106
4.4.3	Identification of Chloromethyl and Amines Groups	108
4.4.4	Evaluation of the Transesterification of Triacetin.....	111
4.4.5	Summary.....	112
4.5	Synthesized Ion Exchange Resins (SIERs).....	113
4.5.1	Synthesis by Aqueous Suspension Polymerization.....	113
4.5.2	Characterization of SIERs	115
4.5.3	Evaluation of SIERs as Transesterification Catalysts	126
4.5.4	Summary.....	132
4.6	Kinetic Modelling	133
4.6.1	Diffusional Resistance.....	133
4.6.2	Second-Order Kinetic Model	137

4.6.3	Langmuir-Hinshelwood-Hougen-Watson (LHHW) and Eley-Rideal (ER) Kinetic Models	147
4.6.4	Summary.....	152
CONCLUSIONS		153
5.1	Conclusions.....	153
5.1.1	GC Analysis of Esters	153
5.1.2	Evaluation of Quaternary Ammonium Ion Exchange Resin as a Heterogeneous Transesterification Catalyst for Rapeseed Oil	153
5.1.3	Quaternary Ammonium as Transesterification Catalysts.....	154
5.1.4	Synthesized Ion Exchange Resins (SIERs)	155
5.1.5	Kinetic Modelling.....	156
FURTHER WORK.....		158
6.1	Further Work.....	158
REFERENCES		160
Appendix 1		175
Appendix 2		185
Appendix 3		189

List of Figures

Figure 1.1: Biodiesel Consumption in the European Union (Mekhilef <i>et al.</i> , 2011)	3
Figure 1.2: Biodiesel Process Scheme (Gerpen, 2005)	7
Figure 1.3: Intensified Biodiesel Process Using Heterogeneous Catalyst.....	8
Figure 2.1: Fatty Acid Distribution of Three Biodiesels (BDs) (Park <i>et al.</i> , 2008)	12
Figure 2.2: Triacetin Chemical Structure	12
Figure 2.3: Stages of the Transesterification Reaction.....	15
Figure 2.4: Overall Transesterification Reaction	15
Figure 2.5: Esterification Reaction of Free Fatty Acid with Methanol (Lotero <i>et al.</i> , 2006)	17
Figure 2.6: (a) Reaction of NaOH or CH ₃ ONa with Free Fatty Acids to Produce Soap and Water; (b) Ester Hydrolysis Due to Reaction with Water Forming Free Fatty Acids (Lotero <i>et al.</i> , 2006).....	20
Figure 2.7: Homogeneous Alkali-Catalyzed Reaction Mechanism for the Transesterification of Triglycerides (Lotero <i>et al.</i> , 2006)	22
Figure 2.8: Mechanism of the Acid-Catalyzed Transesterification of Vegetable Oils (Lotero <i>et al.</i> , 2006).....	25
Figure 2.9: Chemical Structure of Diaion® in Cl ⁻ Ionic Form (Mitsubishi Chemical Corporation, 2003).....	34
Figure 2.10: Polymer Lumps During Polymerization	37
Figure 2.11: Resins in Different Morphology	38
Figure 2.12: Enlarge Macroporous Resin Bead Showing A) Individual Microgel/Microsphere Particles with A ≈ 1000Å (Sherrington, 1998) and B) Bead from SEM Micrograph.....	38
Figure 2.13: Three Stages of Pore Formation in Suspension Polymerization (Sherrington, 1998).....	39
Figure 2.14: Interconnectivity of Microgel Particles within Macroporous Resin Beads (Miguel <i>et al.</i> , 2003).....	42
Figure 2.15: Structure of Vinylbenzyl Chloride	43
Figure 2.16: Langmuir-Hinshelwood-Hougen-Watson (LHHW) Mechanism	53
Figure 2.17: Eley-Rideal (ER) Mechanism	57
Figure 2.18: A Basic Stirred Tank Design With Two Equally Spaced Baffles (Not to Scale), Showing a Lower Radial Impeller and an Upper Axial Impeller. H = Height of Liquid Level, D_t = Tank Diameter, d = Impeller Diameter (Perry and Walas, 1997).....	59
Figure 2.19: Effectiveness Factor Versus M_T for A Porous Particle (Levenspiel, 1999).....	60
Figure 3.1: A Batch Reactor Used in Kinetics Study	68
Figure 3.2: Reusability and Residual Activity Studies.....	70
Figure 3.3: Setup Diagram for Ion Exchange Capacity Analysis.....	73
Figure 3.4: Setup Diagram for Apparent Density Analysis	74

Figure 3.5: Element in the Morphology of Macroporous Resin. A – Swollen Polymer Matrix, B – True Pore (Jerabek, 1996).....	77
Figure 4.1: A GC Chromatogram for Ester Method (1 st Peak Methyl Palmitate, 2 nd Peak Methyl Heptadecanoate, 3 rd Peak Methyl Stearate, 4 th Peak Methyl Oleate, 5 th Peak Methyl Linoleate, 6 th Peak Methyl Linolenate).....	83
Figure 4.2: Transesterification Reaction of Triacetin with Methanol (Lopez <i>et al.</i> , 2005).....	84
Figure 4.3: A Typical Chromatogram of Triacetin and its Reaction Products.....	85
Figure 4.4: Calibration Curves for Six Components in Triacetin GC Analysis.....	86
Figure 4.5: Effect of Pre-Swelling Amberlite™ A26 with Methanol.....	90
Figure 4.6: Triacetin Conversion of Different IERs.....	93
Figure 4.7: SEM Micrographs of D1X2 at 39x and 15000x Magnifications.....	95
Figure 4.8: SEM Micrographs of HPA25 at 38x and 10000x Magnifications.....	95
Figure 4.9: ISEC Analysis on Amberlite™ A26.....	97
Figure 4.10: SEM Micrographs for A26 at 50x and 35000x Magnifications.....	97
Figure 4.11: Reusability of Different IERs in the Transesterification of Triacetin.....	98
Figure 4.12: ¹ H NMR Spectrums for D1X2 (above) and A26 (bottom).....	100
Figure 4.13: Conversion versus Time of Various Species for Transesterification of Triacetin using TMAOH.....	100
Figure 4.14: Transesterification of Triacetin at Different Concentration of TMAOH.....	101
Figure 4.15: Changes in Concentration of Triacetin (TAc) and Methyl Acetate (MeAc) at Various Temperatures.....	103
Figure 4.16: Triacetin Conversion at Different Temperatures.....	103
Figure 4.17 : Selectivities of Diacetin (DAc), Monoacetin (MoAc) and Glycerol (Gly) in the Transesterification of Triacetin.....	104
Figure 4.18: FTIR-ATR Spectra of the Unfunctionalized Merrifield Resin.....	108
Figure 4.19: FTIR-ATR Spectra of the Merrifield Resin Functionalized using TMA (0.127mol/g) at 60°C for 4 Days.....	109
Figure 4.20: FTIR-ATR Spectra of the Merrifield Resin Functionalized using TEA (0.634 mol/L) at 30°C for 32h.....	110
Figure 4.21: ¹ H NMR Spectrum of the Merrifield Resin.....	110
Figure 4.22: Triacetin Conversion of Merrifield Resin Aminated with TMA (24h) ...	111
Figure 4.23: ¹ H NMR Spectrum for the Merrifield Resin in Leaching Test.....	112
Figure 4.24: FTIR-ATR Spectra for the Chloromethylated Resin Beads of Different % Initial VBC: (A) 6% and (B) 10%.....	116
Figure 4.25: FTIR-ATR Spectra for: (A) Chloromethylated and (B) Functionalized Resin Beads.....	117
Figure 4.26: Fraction of Unconverted CH ₂ Cl (%) at Different Dilution Degree (%) and Different DVB Content.....	119
Figure 4.27: Pore Diameter of Functionalized Resin Beads at 50% Dilution Degree .	121

Figure 4.28: SEM Micrographs for SIER-2 (100% DD; 25% DVB) at (A) 250x and (B) 1000x Magnifications	122
Figure 4.29: SEM Micrographs for (A) SIER-8 (50% DD; 25% DVB) and (B) SIER-5 (200% DD; 25% DVB) at 1000x Magnifications.....	122
Figure 4.30: SEM Micrographs for (A) SIER-1 (100% DD; 40% DVB) and (B) SIER-3 (100% DD; 10% DVB) at 1000x Magnifications.....	124
Figure 4.31: SEM Micrographs for (A) SIER-6 (200% DD; 10% DVB) and (B) SIER-4 (200% DD; 40% DVB) at 1000x Magnifications.....	125
Figure 4.32: TGA Analysis Result on SIER-6	126
Figure 4.33: SEM Micrographs for SIER-7 (50% DD; 40% DVB) at 1000x and 35000x Magnifications	128
Figure 4.34: Relation of Site Density to DVB Content (%) at Different Dilution Degree	128
Figure 4.35: Changes in Concentrations of Various Species in the Transesterification of Triacetin using SIER-6	129
Figure 4.36: Selectivities for Diacetin (DAc), Monoacetin (MoAc) and Glycerol (Gly) in the Transesterification of Triacetin using SIER-6	130
Figure 4.37: Reusability of SIER-3 in the Transesterification of Triacetin	131
Figure 4.38: ¹ H NMR Spectrum for SIER-3	131
Figure 4.39: Effect of Agitation Rate on Triacetin Conversion Using 0.6875 mmol/L TMAOH.....	134
Figure 4.40: Effect of Agitation Rate on Triacetin Conversion Using 5.5 mmol Active Sites of D1X4.....	136
Figure 4.41: Variation of Triacetin Conversion using D1X4 at Different Particle Size	136
Figure 4.42: Second-Order Model Fitted to 5.5 mmol/L TMAOH (Methanol) (Line = Model Data; Symbol = Experimental Data)	139
Figure 4.43: Second-Order Model Fitted to 5.5 mmol/L TMAOH (All Compounds Except Methanol) (Lines = Model Data; Symbols = Experimental Data)	139
Figure 4.44: Second-Order Model Fitted to 2.75 mmol/L TMAOH (Methanol) (Line = Model Data; Symbol = Experimental Data)	140
Figure 4.45: Second-Order Model Fitted to 2.75 mmol/L TMAOH (All Compounds Except Methanol) (Lines = Model Data; Symbols = Experimental Data)	141
Figure 4.46: Second-Order Model Fitted to 22 mmol Active Sites of D1X2 (Methanol) (Line = Model Data; Symbol = Experimental Data)	143
Figure 4.47: Second-Order Model Fitted to 22 mmol Active Sites of D1X4 (All Compounds Except Methanol) (Lines = Model Data; Symbols = Experimental Data)	143
Figure 4.48: Second-Order Model Fitted to 5.5 mmol Active Sites of D1X2 (Methanol) (Line = Model Data; Symbol = Experimental Data)	144

Figure 4.49: Second-Order Model Fitted to 5.5 mmol Active Sites of D1X4 (All Compounds Except Methanol) (Lines = Model Data; Symbols = Experimental Data)	144
Figure 4.50: Second-Order Model Fitted to 5.5 mmol Active Sites of SIER-6 (Methanol) (Line = Model Data; Symbol = Experimental Data)	145
Figure 4.51: Second-Order Model Fitted to 5.5 mmol Active Sites of SIER-6 (All Compounds Except Methanol) (Lines = Model Data; Symbols = Experimental Data)	145
Figure 4.52: Second-Order Model Fitted to 5.5 mmol Active Sites of SIER-3 (Methanol) (Line = Model Data; Symbol = Experimental Data)	146
Figure 4.53: Second-Order Model Fitted to 5.5 mmol Active Sites of SIER-3 (All Compounds Except Methanol) (Lines = Model Data; Symbols = Experimental Data)	146
Figure 4.54: ER Model Fitted to 5.5 mmol Active Sites of SIER-6 (Methanol) (Line = Model Data; Symbol = Experimental Data)	148
Figure 4.55: ER Model Fitted to 5.5 mmol Active Sites of SIER-6 (All Compounds Except Methanol) (Lines = Model Data; Symbols = Experimental Data)	149
Figure 4.56: LHHW Model Fitted to 5.5 mmol Active Sites of SIER-6 (Methanol) (Line = Model Data; Symbol = Experimental Data)	149
Figure 4.57: LHHW Model Fitted to 5.5 mmol Active Sites of SIER-6 (All Compounds Except Methanol) (Lines = Model Data; Symbols = Experimental Data)	150
Figure 4.58: ER Model Fitted to 5.5 mmol Active Sites of SIER-6 (Methanol) using $K = 30 \text{ Lmol}^{-1}$ for Glycerol (Line = Model Data; Symbol = Experimental Data)	151
Figure 4.59: ER Model Fitted to 5.5 mmol Active Sites of SIER-6 (All Compounds Except Methanol) using $K = 30 \text{ Lmol}^{-1}$ for Glycerol (Lines = Model Data; Symbols = Experimental Data)	151

List of Tables

Table 1.1: Fatty Acid Composition of Several Vegetable Oils (Goering <i>et al.</i> , 1982)	5
Table 2.1: Physicochemical Properties of Triacetin at 25°C (www.inchem.org, 2002)	13
Table 2.2: Overview of the Heterogeneous Alkaline Catalysts.....	27
Table 2.3: Overview of the Heterogeneous Acid Catalysts	31
Table 2.4: Typical Diluents for S-DVB Copolymers (^a Rabelo and Coutinho, 1994; Sherrington, 1998)	40
Table 2.5: Rate Constant Values for the Forward Reaction	49
Table 4.1: Physicochemical Properties of Amberlite™ A26 (Liu <i>et al.</i> , 2007)	89
Table 4.2: Physicochemical properties of the fresh IER catalysts	92
Table 4.3: Turn Over Frequency of the IERs	94
Table 4.4: Properties of Amberlite™ A26 (Rohm and Haas, 2003)	96
Table 4.5: Progress of Transesterification After Removal of IERs.....	99
Table 4.6: Effect of Amination Reaction Time using TEA at 0.127 mol/g	107
Table 4.7: Effect of Amination Reaction Time using TMA at 0.127 mol/g	107
Table 4.8: Final Recipe for Synthesis of IERs	114
Table 4.9: Composition of the IERs Samples and the Residual Chlorine Determined After Elemental Analysis.....	118
Table 4.10: Comparison of the Dead Volume Obtained from ISEC Analysis.....	120
Table 4.11: Physicochemical Properties of the SIER Catalysts	120
Table 4.12: Site Density and Triacetin Conversion for the SIERs.....	127
Table 4.13: Second-Order Rate Constants Fitted to Experimental Data of 5.5 mmol/L TMAOH.....	138
Table 4.14: Second-Order Rate Constants Fitted to Experimental Data of 2.75 mmol/L TMAOH.....	140
Table 4.15: Second-Order Rate Constants Fitted to Experimental Data of Ion Exchange Resins.....	142
Table 4.16: Rate Constant Values Fitted to Second-Order, Eley-Rideal (ER) and Langmuir-Hinshelwood-Hougen-Watson (LHHW) Models for 5.5 mmol Active Sites of SIER-6	148
Table 4.17: Individual Sum of Square Errors of ER and LHHW Models for 5.5 mmol Active Sites of SIER-6.....	148

Nomenclature and Abbreviations

Symbols

D	molecular diffusion coefficient (m^2/s),
K	adsorption coefficient (Lmol^{-1})
k_1	forward rate constant for the reaction of triglyceride to diglyceride ($\text{Lmol}^{-1} \text{min}^{-1}$)
k_2	backward rate constant for the reaction of triglyceride to diglyceride ($\text{Lmol}^{-1} \text{min}^{-1}$)
k_3	forward rate constant for the reaction of diglyceride to monoglyceride ($\text{Lmol}^{-1} \text{min}^{-1}$)
k_4	backward rate constant for the reaction of diglyceride to monoglyceride ($\text{Lmol}^{-1} \text{min}^{-1}$)
k_5	forward rate constant for the reaction of monoglyceride to glycerol ($\text{Lmol}^{-1} \text{min}^{-1}$)
k_6	backward rate constant for the reaction of monoglyceride to glycerol ($\text{Lmol}^{-1} \text{min}^{-1}$)
M_T	Thiele Modulus
Re	Reynolds Number
V	true pore volume (cm^3/g)
ε_p	catalyst particle porosity
τ_p	catalyst particle tortuosity

Abbreviations

AgNO_3	silver nitrate
AIBN	2,2'-azobis(2-methylpropionitrile)
ASTM	American Standards for Testing of Materials
ATR	Attenuated Total Reflectance
BDs	Biodiesels
BPO	Benzoyl peroxide
$\text{C}_2\text{H}_4\text{Cl}_2\text{O}$	Bischloromethyl ether
$\text{C}_2\text{H}_5\text{ClO}$	Chloromethyl methyl ether
$\text{C}_3\text{H}_7\text{NO}$	Dimethylformide
$\text{C}_9\text{H}_{14}\text{O}_6$	Triacetin
$\text{C}_9\text{H}_9\text{Cl}$	Chloromethyl styrene
CaO	Calcium oxide
CD_3OD	Deuterated methanol
CFPP	Cold Filter Plugging Point
CP	Cloud Point
DAc	Diacetin
DCSG	1,3-dicyclohexyl-2-sec-butyl-guanidine
DD	Dilution Degrees
DG	Diglyceride
DMF	Dimethylformamide
DVB	Divinylbenzene

ER	Eley-Rideal
FAME	Fatty Acid Methyl Ester
FAO	Food & Agriculture Organization
FFAs	Free Fatty Acids
FID	Flame Ionisation Detector
FTIR	Fourier Transform Infrared Spectroscopy
GC	Gas Chromatography
H ₂ SO ₄	Sulphuric acid
HCl	Hydrochloric acid
HEC	Hydroxyethyl cellulose
HIPE	High Internal Phase Emulsion
HNO ₃	Nitric acid
HPLC	High Performance Liquid Chromatography
IEC	Ion Exchange Capacity
IERs	Ion Exchange Resins
IPA	Isopropyl alcohol
ISEC	Inverse Steric Exclusion Chromatography
KOH	Potassium hydroxide
LHHW	Langmuir-Hinshelwood-Hougen-Watson
MeAc	Methyl acetate
MeOH	Methanol
MG	Monoglyceride
MHDN	Methyl heptadecanoate
MoAc	Monoacetin
NaCl	Sodium chloride
NaOH	Sodium hydroxide
NH ₄ OH	Ammonium hydroxide
NMR	Nuclear Magnetic Resonance
PEG	Polyethylene glycol
PVOH	Polyvinyl alcohol
QN ⁺ OH ⁻	Quaternary ammonium functional group
RDS	Rate-Determining Step
RTFO	Renewable Transport Fuel Obligation
S-DVB	Styrene-divinylbenzene
SEM	Scanning Electron Microscope
SIERs	Synthesis of Ion Exchange Resins
SSE	Sum of Square Error
TBD	1,5,7-Triazabicyclo [4.4.0] dec-5-ene
TCG	1,2,3-Tricyclohexylguanidine
TEA	Triethylamine
TG	Triglyceride
TGA	Thermal Gravimetric Analysis
THF	Tetrahydrofuran
TMA	Trimethylamine
TMAOH	Tetramethylammonium hydroxide
TOF	Turnover frequency
VBC	Vinylbenzyl chloride

CHAPTER I

INTRODUCTION

1.1 Background: Biofuels

The current high demand worldwide for transport fuels derived from fossil fuel has largely resulted from the mass production of automobiles, which began early in the 19th century (Hirao and Pefley, 1988). The emissions produced by fossil fuel-based power stations and the growth in the number of automobiles, and the related use of petroleum fuels around the world has led to a steady increase in atmospheric pollution due to exhaust emissions. In 2004, 30% of total carbon dioxide discharges in the United Kingdom (UK) were from the transport sector, and this sector has the fastest growing rate of emissions (Hammond *et al.*, 2008). Despite a UK government target to reduce such emissions by 2010, an increase of 7.5% in carbon emissions was recorded between 1995 and 2005, accounting for 120.1 million tonnes of carbon dioxide emissions from road transport in the UK (Department for Transport, 2007).

Fossil fuel deposits used to produce diesel and gasoline are likely to run out within a century (Ranganathan *et al.*, 2008). The high demand for these finite reserves has recently led to steep worldwide increases in fossil fuel prices, adversely affecting the economic stability of countries that import crude petroleum, including the UK. In addition, the risk of potential disruptions in the supply of petroleum due to the political instability of some major exporting countries, especially in the Middle East, will also influence supply. This dependence on fossil fuels constitutes a threat to European Union (EU) and UK competitiveness (Lin *et al.*, 2011).

The contribution of fossil fuels to the accumulation of carbon dioxide in the environment, as well as the drive for future UK competitiveness, have encouraged the use of alternative fuels, which are more “environmental friendly”. It is necessary

to look for alternative fuels that can be produced from local resources. Research into and developments of carbon neutral and renewable fuels have therefore received considerable interest in the scientific community. As energy demands and the price of fossil fuels increase, the search for alternative fuels has gained greater prominence. Liquid fuels derived from biomass using various chemical and biological processes have been identified as possible alternative energy resources. Two types of biofuel whose development has advanced the most are biodiesel and bioethanol. They have already been produced commercially on an industrial scale. Others, such as biomethanol and biobutanol, have been subject to research but are not yet produced commercially (Agarwal, 2007).

Biodiesel derived from vegetable oil, is one type of alternative fuel that could be produced in the UK, since there are abundant local oil crops available as feedstock, such as rapeseed and corn. According to Demirbas (2005), more than 350 oil crops can be used as feedstock for biodiesel. Among these are rapeseed, sunflower, soybean, jatropha, palm oil, and peanut oil. Recent increases in UK crude oil prices, from around £50 per barrel in 2008 to around £62 per barrel in 2011 (Energy Information Administration, 2011), have led to renewed interest in utilizing vegetable oil as a biofuel. Indeed, the use of biodiesel as an alternative fuel could contribute to meeting the growing demand for energy, especially in the UK transport sector, while at the same time reducing carbon dioxide emissions.

There is a need to balance the usage of oil crops as a feedstock, since most such crops in the UK are intended for use in the food industry. The introduction of biodiesel has increased the demand for oil crops, created business opportunities from the use of biomass, and helped agricultural development in the UK. However, without a proper balance between food and fuel, food shortages and price increases may have negative effects on consumers as well as on farmers, most of whom use such crops to feed their livestock. Sustainable agriculture is currently a topic of intense debate, and policy-makers must make difficult decisions to balance future food and energy needs.

Since 2005, the biodiesels market in Europe has grown rapidly to meet the European Biofuels Directive (2003/30/EC) target of 5.75% by volume of biofuels to be used in the transport sector by 2010. In the UK itself, biodiesel consumption in 2006 has

increased more than five fold compared to 2005, as can be seen in Figure 1.1, before doubling by 2007. However, it has been reported that by 2010, the majority of EU members had been unable to reach the target. Because of this, the Renewable Energy Directive (2009/28/EC) came into force in 2011, replacing the Biofuels Directive, and introducing the mandatory use of renewable energy in the EU transport sector. The Renewable Energy Directive target for the UK is to achieve 15% of its energy consumption from renewable resources by 2020 (European Commission Energy, 2011).

Country	Year 2005 (tonnes)	Year 2006 (tonnes)	Year 2007 (tonnes)	Year 2008 (tonnes)
Germany	209	342	393	335
France	46.6	80	164	273
United Kingdom	3.4	18	37	94
Italy	23.3	20	18	75
Spain	3.1	7.32	35	70
Poland	1.8	5.71	3.38	46
Netherlands	0	2	30	27
Austria	10.7	45	26	25
Portugal	0	9.51	18	18
Sweden	1.1	6.08	14	18
Belgium	0	0.12	12	12
Hungary	0	0.05	0.27	10.96
Czech Republic	0.4	2.48	3.8	10.25
Greece	0.4	6.28	10.99	10.23
Romania	0	0.37	5.41	8.14
Slovenia	0.7	0.56	10.42	7.18
Lithuania	1	1.88	5.69	6.19
Luxembourg	0.1	0.07	5.63	5.61
Ireland	0.1	0.09	2.34	5.41
Slovenia	1.3	1.73	1.76	3.01
Cyprus	0	0	0.1	1.92
Finland	0	0	0.01	1.55
Estonia	0	0.08	0.07	0.37
Latvia	0.3	0.2	0.23	0.26
Malta	0.1	0.12	0.24	0.13
European Union	304	551	798	1.069

Figure 1.1: Biodiesel Consumption in the European Union (Mekhilef *et al.*, 2011)

Another contributing factor to the observed increase in biofuel usage has been the implementation of the Renewable Transport Fuel Obligation (RTFO) by the Department of Transport since April 2008. This is intended to deliver reductions in carbon dioxide emissions from the road transport sector of 2.6 to 3.0 million tonnes per annum (equivalent to carbon savings of 700,000 to 800,000 tonnes) by 2010, by encouraging the supply of renewable fuels. Previously, the RTFO had required 2.5%, 3.75% and 5% by volume of all fuel sold on UK forecourts to be renewable by 2008, 2009 and 2010, respectively (Department of Transport, 2008). However, in January 2009 the RTFO programme was revised upward to 3.25%, 3.5%, 4.0%, 4.5%, and 5.0% by volume of all fuel sold on UK forecourts to be renewable by

2009/10, 2010/11, 2011/12, 2012/13, and 2013/14, respectively (Department of Transport, 2009).

1.2 The Use of Vegetable Oils

The use of vegetable oil as a fuel began first became possible after invention by Rudolph Diesel of an engine based on compression ignition (Pinto *et al.*, 2005). In 1900, Diesel's engine was unveiled at the World Fair held in Paris, running on a variety of peanut oil (Mittelbach and Remschmidt, 2006). For various reasons, only a limited range of vegetable oils have been favoured as biodiesel feedstocks. One of the most significant is rapeseed oil (*Brassica napus*), which was originally chosen because of its low price compared to other readily available vegetable oils. It turned out to be an ideal feedstock in terms of combustion characteristics, oxidation stability, and low temperature behaviour, as explained below in section 2.2.1. Until now, it has remained the feedstock of choice in most European countries due to these properties (Mittelbach and Remschmidt, 2006).

It is possible to use vegetable oil directly to power diesel engines by simply blending it with diesel fossil fuels at an appropriate ratio. However, these blends are stable only for short-term usage due to their high viscosity, acid contamination, free fatty acid formation (resulting in gum formation by oxidation and polymerization) and carbon deposition (Ranganathan *et al.*, 2008). In addition, there are several other problems associated with the direct use of vegetable oils, especially in direct injection engines. These include (Meher *et al.*, 2006):

- i) Coking formation on the injectors to such an extent that fuel atomization does not occur properly or is even prevented as a result of plugged orifices;
- ii) Carbon deposits on the piston and head of the engine;
- iii) Oil ring sticking;
- iv) Thickening or gelling of the lubricating oil as a result of contamination by vegetable oils; and
- v) Lubricating problems due to polymerization.

Table 1.1 below shows the fatty acid composition of several vegetable oils (Goering *et al.*, 1982). It should be noted that rapeseed oil is rich in unsaturated fatty acid,

comprised of C18:1 (oleic acid), C18:2 (linoleic acid), C18:3 (α -linoleonic acid) and C16:1 (palmitoleic acid), and a small amount of saturated acid (stearic acid, C18:0; also known as ‘octadecanoic acid’).

Table 1.1: Fatty Acid Composition of Several Vegetable Oils (Goering *et al.*, 1982)

Fatty acid composition												
Vegetable oil	Fatty acid composition % by weight									Acid value	Phos (ppm)	Peroxide value
	16:1	18:0	20:0	22:0	24:0	18:1	22:1	18:2	18:3			
Corn	11.67	1.85	0.24	0.00	0.00	25.16	0.00	60.60	0.48	0.11	7	18.4
Cottonseed	28.33	0.89	0.00	0.00	0.00	13.27	0.00	57.51	0.00	0.07	8	64.8
Crambe	20.7	0.70	2.09	0.80	1.12	18.86	58.51	9.00	6.85	0.36	12	26.5
Peanut	11.38	2.39	1.32	2.52	1.23	48.28	0.00	31.95	0.93	0.20	9	82.7
Rapeseed	3.49	0.85	0.00	0.00	0.00	64.4	0.00	22.30	8.23	1.14	18	30.2
Soybean	11.75	3.15	0.00	0.00	0.00	23.26	0.00	55.53	6.31	0.20	32	44.5
Sunflower	6.08	3.26	0.00	0.00	0.00	16.93	0.00	73.73	0.00	0.15	15	10.7

In order for the use of vegetable oil to be practical, it needs to be processed to meet the primary criteria for biodiesel quality represented by adherence to the appropriate standards. Examples of such standards are those set up by the American Standards for Testing of Materials D 6751-02 (ASTM, 2002) in the US and the British Standards Institution BS EN 14214 (BSI, 2003) in the UK, which is identical to the European Standard EN 14214:2003. There are three processing techniques that are used to convert vegetable oil into biodiesel, which are discussed in detail by Ma and Hanna (1999) and Fukuda *et al.* (2001). Those processes are pyrolysis, microemulsification and transesterification.

Pyrolysis, also known as cracking, refers to a process of thermochemical decomposition with the aid of a catalyst to simplify the chemical compounds in the vegetable oil. This process involves heating in the absence of oxygen, resulting in cleavage of chemical bonds to yield small molecules. This lowers the viscosity of the oils and at the same time increases their cetane number thus improving ignition quality. However, problems with this technique include the high cost of equipment (Ma and Hanna, 1999).

Microemulsification involves the formation of thermodynamically stable dispersions of two usually immiscible liquids, brought about by one or more surfactants (Mittlebach and Remschmidt, 2006). The microemulsification technique is able to

lower the viscosity of vegetable oils using solvents such as methanol, ethanol and 1-butanol (Fukuda *et al.*, 2001). However, microemulsification with alcohols is not recommended for long-term use in diesel engines, due to problems of injector needle sticking, incomplete combustion, heavy carbon deposition, and an increase in the viscosity of the lubricating oil (Ziejewski *et al.*, 1984).

The third technique used is the transesterification reaction, where one ester is transformed into another through the interchange of the alkoxy moiety (Schuchardt *et al.*, 1998). In biodiesel production, transesterification involves the reaction between the triglyceride molecules in the vegetable oils and alcohol in the presence of a catalyst to produce monoesters. This technique is also known as alcoholysis, since the ester is split using alcohol. The long, branched chain triglyceride molecules are transformed into linear monoesters and glycerol. This topic is discussed in detail below in section 2.3.1.

1.3 Intensified Biodiesel Process Using Heterogeneous Catalyst

Different types of catalyst can be used to synthesize biodiesel, including homogeneous or heterogeneous base-catalysts and acid-catalysts, and biocatalysts. However, most commercial biodiesel processes use homogeneous base catalysts for transesterification, since the reaction proceeds at a much higher rate than when homogeneous acid catalysts are used (Ma and Hanna, 1999; Kim *et al.*, 2004). In addition, the base catalysts are less corrosive than acidic compounds, making them more favourable for industrial processes. Currently, most biodiesel is produced by the transesterification of triglycerides from waste cooking oil and edible or non-edible oils using methanol as a solvent. Nearly all the processes use homogeneous base catalysts, such as alkaline metal alkoxides (CH_3ONa), hydroxides (NaOH and KOH), and carbonates (Na_2CO_3 and K_2CO_3), since they give conversion rates to biodiesel of over 95% (Schuchardt *et al.*, 1998; Rashid and Anwar, 2008).

Even though reproduction of biodiesel using homogeneous base-catalysts involves a rapid process resulting in high conversion rates with minimal side reactions, it is still not very commercially competitive compared to petroleum diesel due the factors listed below (Lopez *et al.*, 2005):

- i) the catalyst cannot be recovered;
- ii) the use of homogeneous catalyst necessitates the neutralization of glycerol at the end of the reaction;
- iii) there is limited use of continuous processing methodologies; and
- iv) the processes involved are very sensitive to the presence of water and free fatty acids.

Figure 1.2 below shows a schematic diagram of the conventional process using a homogeneous catalyst in biodiesel production (Gerpen, 2005). At the beginning of the process, alcohol, oil, and catalyst are combined in a reactor and agitated for approximately an hour at 60°C. After transesterification, the reaction mixture separates spontaneously into two layers, although complete separation requires a longer period of settling. The top layer containing esters and methanol has to be separated and the esters are then neutralized and washed with water to remove free glycerol. After that it has to be dried to obtain a pure biodiesel. The bottom layer containing glycerol needs to be neutralized in order to remove the catalyst residue.

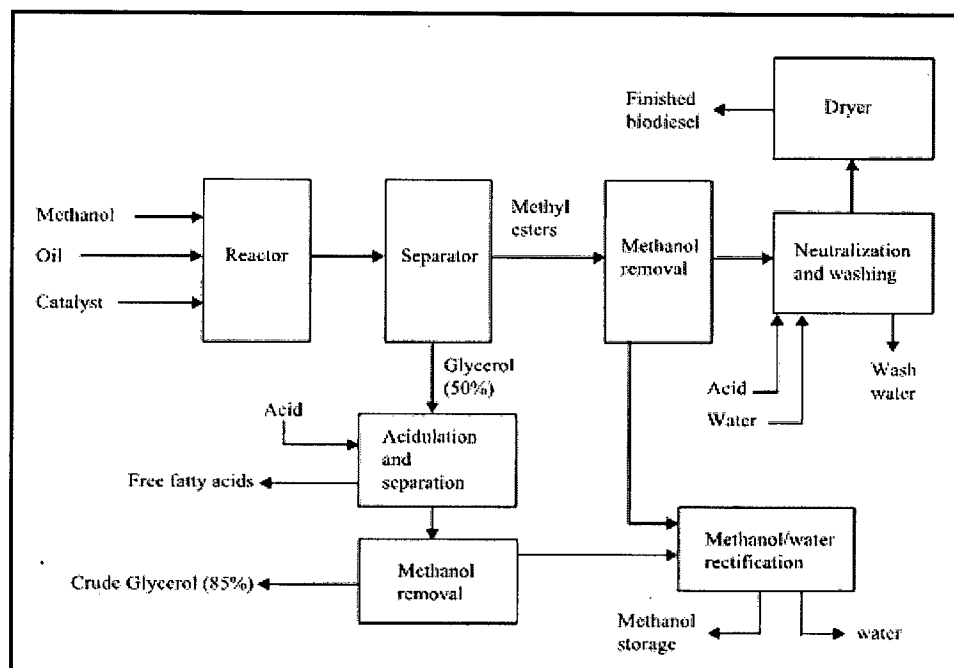


Figure 1.2: Biodiesel Process Scheme (Gerpen, 2005)

The intensified biodiesel process using heterogeneous catalysts is shown in Figure 1.3 below. As can be seen, replacing liquid homogeneous catalysts with solid heterogeneous catalysts is expected to yield a product that does not require neutralization, leading to lower processing costs, because the catalyst will not have

to be continually replaced. The separation of solid heterogeneous catalysts can be easily achieved by filtration, and production costs could be reduced by using intensified operations and eliminating waste streams. However, the chemical stability of heterogeneous catalyst is likely to play a major role in determining their capability to be reliably reusable.

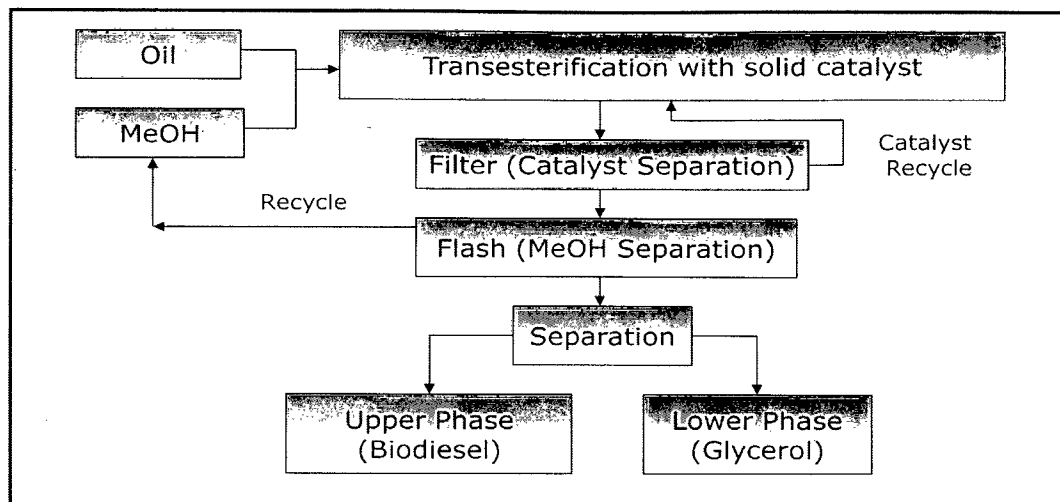


Figure 1.3: Intensified Biodiesel Process Using Heterogeneous Catalyst

The use of a heterogeneous catalyst on an industrial scale has been described by Di Serio *et al.*, (2008). The 160 000 tonnes/year biodiesel plant operated in France by the Institute Francais du Pétrole (IFP) is based on the Esterfip-HTM technology where the catalyst employed is a mixed oxide of zinc and aluminum, which promotes the transesterification reaction without catalyst loss. However, this technology operates at 200°C to 250°C, which is much higher than in conventional methods that usually run near the boiling point of methanol, according to most studies. It also requires high pressure and an excess of methanol, which is removed by vaporization and recycled back into the process along with fresh methanol (Bournay *et al.*, 2005).

Several types of heterogeneous base catalysts have been developed for the transesterification of vegetable oils into biodiesel over the past few years, as discussed in depth in section 2.4.2 in the literature review. Among these, solid Brønsted base catalysts with a quaternary ammonium functional group (QN⁺OH⁻) have been identified as an alternative to homogeneous base catalysts that suitable for transesterification in biodiesel production, due to their stability and the better conversion rates achieved (Liu *et al.*, 2007; Shibasaki-Kitakawa *et al.*, 2007).

However, no published study has investigated the use of homogeneous base catalysts with quaternary ammonium functionality (QN^+OH^-), for the transesterification of vegetable oils into fatty acid methyl esters, as comparison. This is addressed in this study.

1.4 Research Objective

The objective of this research was to develop and evaluate the use of an anion exchange resin with quaternary ammonium functional groups (QN^+OH^-), as a heterogeneous base catalyst for the mild temperature transesterification of triglycerides using methanol as the solvent.

1.5 Research Scope

To achieve the objective of this study, four research aims were identified:

- a) To examine the performance of homogeneous and heterogeneous base catalysts with the quaternary ammonium functional groups (QN^+OH^-) in the transesterification of triglycerides.
- b) To evaluate the reusability of heterogeneous base catalysts in the transesterification of triglycerides.
- c) To develop a kinetic model of transesterification in order to investigate its mechanisms.
- d) To synthesize and characterize an anion exchange resin with quaternary ammonium functional groups (QN^+OH^-) and to evaluate its performance and reusability.

CHAPTER II

LITERATURE REVIEW

2.1 Introduction

This literature review begins with an introduction to the feedstock and triglycerides used in this study, namely rapeseed oil and triacetin. Rapeseed oil was chosen because it is the main feedstock used in biodiesel production in Europe and particularly in the UK. Triacetin was used as a model triglyceride since it allows reactions to reach completion within a practical time frame, and the reactants and products are easily monitored and quantified.

Next, the transesterification and esterification reactions are described. The homogeneous or heterogeneous catalysts commonly involved in transesterification forms are also discussed. Since the study involved the synthesis of ion exchange resins, various methods for achieving this are described. Finally, the reaction kinetics and modelling to evaluate the performance of catalyst are discussed.

2.2 Sources of Triglycerides

2.2.1 Rapeseed Oil

Oils and fats belong to a large class of compounds known as lipids, which are known for their energy storage capacity. Lipids are usually hydrophobic and can easily dissolve in organic solvents. Normally, animals produce more fats, while plants produce more oils. Both oils and fats consist mainly of triglyceride molecules, which are triesters of glycerol and free fatty acids (Lotero *et al.*, 2006).

After soybean and palm oil, rapeseed is the third most abundant source of vegetable oil in the world and, along with sunflower oil is a major vegetable oil feedstock for

biodiesel production in Europe (Piazza and Foglia, 2001). Rapeseed oil from oil seed rape (*Brassica napus* L. ssp. *oleifera*) also known as rape oil, colza oil or canola oil ('Canadian Oilseed Low Acid'), originated in Northern Europe. Rapeseed or colza oil in large doses can cause serious damage to the human liver and heart due to its high levels of erucic acid which is around 50%. It also contains compounds known as glycosinolates, which are toxic to humans and animals. Because of this, new plant breeds were developed from the 1960s onwards by Canadian biologists to produce 'canola oil', which has lower levels of erucic acid and trace amounts of glucosinolates (Mittelbach and Remschmidt, 2006).

Rapeseed oil has been used since the early 13th century, in Europe as a lamp oil, a raw material for soap and paint production and cheap cooking oil. It is now in high demand for the production of animal feed, vegetable oil, and biodiesel and has been widely cultivated throughout the world. Presently, the largest modern growers are China, Canada, and India (Food & Agriculture Organization, 2008). The production of rapeseed has increased globally since the early 1960s, reaching a peak in 1999 of 43.2 million metric tons (Mead *et al.*, 2008). However, production is currently increasing again, and the Food & Agriculture Organization reported that world production of rapeseed oil stood at 46.4 million tonnes in 2005 (Food & Agriculture Organization, 2008).

The most favourable characteristic of rapeseed oil as a biodiesel feedstock is the high oil content in the seed of 40% to 45% (Mittelbach and Remschmidt, 2006) along with their chemical properties as detailed in Figure 2.1, which contribute to the quality of the biodiesel produced by affecting the cold flow properties. These are related to the cloud point (CP) and cold filter plugging point (CFPP). The former indicate the temperature at which small wax crystals (approximately 0.5 mm in width) are formed, representing the beginning of the crystallization of fatty acid methyl ester (FAME), of saturated fatty acids; whereas the later shows the temperature at which the fuel tends to jam the filter due to the formation of agglomerations of crystals (Kazancev *et al.*, 2006).